Journal Pre-proofs

Research paper

Non-twisted stacks of coated conductors for magnets: analysis of inductance and AC losses

Davide Uglietti, Rui Kang, Rainer Wesche, Francesco Grilli

Please cite this article as: Uglietti, D., Kang, R., Wesche, R., Grilli, F., Non-twisted stacks of coated conductors for magnets: analysis of inductance and AC losses, *Cryogenics* (2020), doi: https://doi.org/10.1016/j.cryogenics.2020.103118

This is a PDF file of an article that has undergone enhancements after acceptance, such as the addition of a cover page and metadata, and formatting for readability, but it is not yet the definitive version of record. This version will undergo additional copyediting, typesetting and review before it is published in its final form, but we are providing this version to give early visibility of the article. Please note that, during the production process, errors may be discovered which could affect the content, and all legal disclaimers that apply to the journal pertain.
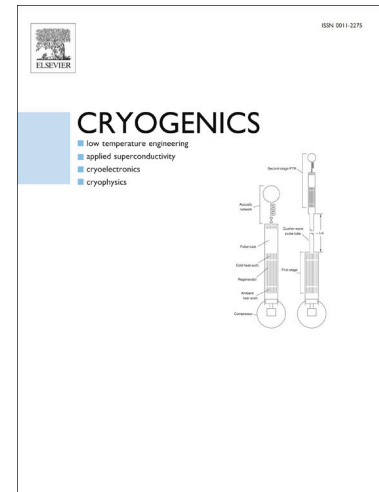
Non-twisted stacks of coated conductors for magnets: analysis of inductance and AC losses

Davide Uglietti[a]*, Rui Kang[a,b], Rainer Wesche[a], Francesco Grilli[c]
[a] Ecole Polytechnique Fédérale de Lausanne (EPFL), Swiss Plasma Center (SPC), CH-5232 Villigen PSI, Switzerland
[b] Department of Engineering and Applied Physics, University of Science and Technology of China, Hefei 230026, China
[c] Karlsruhe Institute of Technology, Karlsruhe, Germany
* Corresponding author. E-mail address: davide.uglietti@psi.ch

Abstract – Almost all present High Temperature Superconducting (HTS) cable designs for magnets are based on twisted or transposed concepts that were developed for Low Temperature Superconducting (LTS) cables. However, requirements for LTS materials (like filament twisting) are in general not valid for HTS materials, which are extremely stable; for example, non-twisted multifilamentary Bi-2223 tapes have been successfully used in several magnets. Is twisting necessary for HTS cables? We investigated inductance mismatches and AC losses by numerical and analytical methods in twisted and non-twisted stacks of coated conductors; various experiments reported in the literature support the analysis. Large (hysteretic) losses are common in all magnets built with tapes and are far larger than in magnets built with LTS multifilamentary conductors, because of the aspect ratio and large width of the tape. In small magnets, losses and residual magnetisation could be reduced by replacing a wide tape with a non-twisted stack of narrow tapes. In large cables, we have found that twisting a stack of tapes reduces losses only marginally. Therefore, non-twisted stack cables could be designed to have losses comparable to those of twisted ones. Some examples of non-twisted large cables for fusion applications are discussed: non-twisted stack designs can be simpler, more robust and cost effective than twisted ones, but would require additional R&D.

1. Introduction

Cable and conductors made of RE-Ba$_2$Cu$_3$O$_{7-\delta}$ (REBCO) tapes have attracted more and more interest in the last 10-15 years, see reviews [1], [2] and [3]. Most of the proposed REBCO cable designs imitate the twisted/transposed concepts that were developed for LTS cables in the 70's and 80's (see [4] for a review of LTS fusion cables and conductors). Therefore, it is important to discuss the reasons that guided the design of LTS cables and whether their requirements should be used also for HTS materials.

In the 50's and 60's, the main obstacle to the construction of superconducting magnets was the low stability of LTS materials. The solution was to subdivide the superconducting material in very fine twisted filaments, embedded in a low resistance matrix. When large currents were needed, it was found that simply winding several strands in parallel would lead again to instability, because the strands would be fully coupled, behaving like a large monolithic conductor. An example is the conductor of the T-7 magnet [5], which was composed of several parallel NbTi strands. This magnet reached only 90% of the expected performance, due to flux jumps and large saturated losses. To avoid that, twisted/transposed designs were developed during the 70's and 80's.

There are few exceptions to the rule of twisted/transposed conductor: 1) The LIN-5 conductor [6], which is composed of 25 parallel NbZr wires arranged in a ribbon-like conductor. 2) The IMP mirror coils [7], which were wound with a 2.9 mm x 1.4 mm conductor composed of 15 NbTi parallel strands in copper matrix. For both magnets, no operating anomalies were reported. 3) In the last decades, many magnets have been built with Bi$_2$Sr$_2$Ca$_2$Cu$_3$O$_x$ (Bi-2223) tapes and have been successfully operated. Filaments in high current density Bi-2223 tapes are parallel (non-twisted). If this configuration was applied to LTS tapes, it would likely lead to flux jump and saturated loss instabilities, like in the T-7 conductor.

These few examples challenge the obligation to twist and/or transpose elements in superconducting conductors, and trigger some questions: if Bi-2223 tapes (non-twisted filaments) can be used in magnets, why cannot a non-twisted stack of two or three coated conductor tapes be used? If those non-twisted conductors worked because of the small size, what is the maximum size for non-twisted conductors? These questions regards not only strands, but also cables and conductors. The distinction between strand and cables is only a convention about the manufacturing process. The physics (for example AC loss and inductance) is the same.

This paper tries to examine the reasons for twisted and transposed HTS cable. The main objections against non-twisted conductors are stability, variation in inductance (leading to current unbalance) and AC losses. In section 2, stability in LTS and HTS magnets is reviewed. In section 3 the inductance variation in the so-called "partially transposed" cables, like twisted and non-twisted stacks of coated conductors, is studied. In section 4 losses in twisted and non-twisted conductors are introduced. Section 5 discusses examples of loss estimation and measurement in small solenoids built with single tape and with non-twisted stacks. In section 6 the losses in large cables (twisted and non-twisted stacks of tapes) are compared, considering the application in fusion magnets.

2. Stability in LTS and HTS materials – a brief review

LTS materials have low stability against thermal disturbances. The reason is the very fast decrease of the critical current density, J_c, with temperature and the very steep superconducting transition with temperature. The stability issue was solved by subdividing the superconducting material in fine,

twisted filaments, embedded in a highly conductive matrix (for example high purity copper); twisting of the filaments is required to uncouple them magnetically.

In contrast with LTS, HTS have a larger temperature margin, J_c decreases very slowly with temperature and the transition is smooth; in addition, the large temperature margin and the fact that specific heat grows with T^3 at low temperatures (4.2 K – 10 K) strongly suppress the positive feedback loop leading to quench. Therefore, they are much more stable against thermal disturbances. Indeed, the phenomenology of HTS strands and magnets is completely different from the one of the LTS counterparts:

- "Training" is a common phenomenon observed in most of LTS magnets, and it is due to tiny wire movements or epoxy cracking, whose energy release is sufficient to trigger quenches. Instead, there are no reports (to our knowledge) of training or of quenches by wire movement / epoxy cracking in HTS magnets.

- In LTS filamentary wires, the filament diameter has to be less than few tens of micron to guarantee sufficient stability. These values are obtained using equation 7.7 in [8], page 134:

  $\dfrac{\mu_0 J_c^2 a^2}{3 C_V (T_c - T)} < 1$, where J_c is the critical current density in the superconductor, a the filament diameter, C_V the volumetric specific heat and T_c the critical temperature. When the same formula is applied to HTS (see for example [9] and [10]), the maximum diameter is found to be of the order of mm, orders of magnitude larger than in LTS. In LTS the fine filaments must be twisted

  with a twist pitch shorter than the critical twisting length $L_c = \sqrt{\dfrac{d \rho J_c}{dB/dt}}$ (equation 8.36 in [8], page

  175), where d is the filament thickness, ρ the matrix resistivity, dB/dt the magnetic field sweep rate. If the twist pitch was greater than L_c, the filaments would be magnetically coupled, and stability and AC loss would be similar to the ones of a single filament as large as the wire.

- Flux jumps in tapes: most of the magnets built in 60's and 70' with Nb$_3$Sn tapes reached only 20% to 50% of the field expected from short sample J_c. The reason was flux jump instabilities [11]. To mitigate that, large cross section of high purity (RRR>1000) Al stabilizer had to be added and, even more important, cooling had to be optimal [12]. The flux jump fields in HTS were compared to those of NbTi in [13]: "*With flux jump fields being between one and two orders of magnitude higher than for conventional SC, the necessity for the use of a multi filamentary conductor is greatly relaxed. Therefore HTSC in the form of solid tapes become an attractive option for many applications*". Flux jumps occur when $B > \sqrt{3 \mu_0 C_V (T_c - T_0)}$. At 4.2 K the right term is larger for HTS material because of the higher critical temperature, and it increases even more at high temperatures ($C_V \sim T^3$), leading to the so-called "partial flux jump": the jump dies out before the full conductor becomes normal ([8], page 135). It is not excluded that in certain conditions, flux jumps may occur also in HTS tapes, but they would not trigger a quench. Indeed, so far no HTS magnets have failed to reach its design field because of flux jump instabilities.

- In LTS wires a high conductive matrix (for example copper with RRR>100) must be present and should be in good contact with the filaments; moreover, in some LTS magnets, heat removal had to be very good (leading to cable in conduit concepts). On the contrary, in coated conductors, there are no reports of instabilities, even if the Cu layer is very thin and has a poor RRR (<40) and in conduction cooled magnets (cryogen free).

HTS materials are more stable than LTS at 4.2 K; the stability is even increased at temperatures > 20 K. The microstructure of Bi-2223 tapes, Bi$_2$Sr$_2$CaCu$_3$O$_x$ (Bi-2212) wires and

3

REBCO coated conductors is not determined by stability, but by the maximization of the critical current and the manufacturability in long length. For example, Bi-2223 tapes are composed of filaments because J_c is higher than in a mono-core tape; the reason is the better texturing of the ceramic close to the Ag matrix. It is technically possible to twist the filaments in Bi-2223 tapes (AC loss reduction only at low frequency), but the disadvantages (higher cost, lower J_e) made them uncompetitive.

The countermeasures to wire movement, magnet training, flux jumps, and other instabilities affecting LTS should not be applied "a priori" to HTS, because HTS are intrinsically very resilient to these issues. Therefore, it would be reasonable to expect that the same criteria that have driven the HTS strands development (maximization of J_c) be also used for HTS cable development. Instead, most of the HTS cable designs proposed so far are imitating LTS cable designs. One of the exceptions is the CORC® cable (see [3], section 5.3), which exploits a unique feature of coated conductors (tolerance to large compressive longitudinal strain and asymmetric layout of the tape). Specific featurea of CORC® cables are the high flexibility (small bending radius) and the isotropic behaviour of the critical current. However, it is unclear what the advantages of an isotropic conductor are. Quench protection remains challenging because the tapes remain superconducting even when the temperature margin is exceeded in an isotropic cable.

3. Inductance

The terms "transposition" and "twisting" are used frequently when discussing superconducting cables, but they have different meanings. "Transposed" means that all the strands follow the same trajectory (if strands are translated in longitudinal direction), or, in other words, that the strands periodically swap their positions; it follows that transposed strands have all the same inductance. "Twisted" means that rotation is applied to the strands during cabling. In Rutherford cables and ITER cables, the strands are twisted and transposed. In Roebel cables (or bars), the strands are non-twisted but transposed. Examples of twisting without transposition are: tapes in CORC®, tapes in twisted stacks, strands in the sub-cable of the RW2 conductor for EU-DEMO [14] and even filaments in Nb_3Sn and NbTi wires. The term "partially transposed" is sometimes employed when discussing twisted, non-transposed cables and conductor. However the meaning of "partially transposed" is vague, and is unclear how "partial transposition" should be measured or quantified. Quoting Lord Kelvin: "When you can measure what you are speaking about and express it in numbers, you know something about it", seen at Hunterian Museum, University of Glasgow. How to quantify transposition? In transposed cables, all strands have the same inductance, then the amount of "partial transposition" can be quantified as the variation in inductance among the strands. To our knowledge, only in [15], section 6, the calculation of the inductance variation for a straight, non-twisted stack of tapes has been attempted. The total inductance of tape i in the stack (composed of N tapes) is the sum of the tape self-inductance plus the sum of the mutual inductances between tape i and all other tapes: $L_i = L_{self} + \sum_{j=1, j \neq i}^{N} M_{ij}$. We have repeated the calculation, using equation (9) from [16], p. 35 for the self-inductance. The mutual inductance is obtained considering the first three terms of equation (3) from [16], page 33:

$M_{ij} = 0.002l \left(\log \frac{2l}{GMD_{ij}} - 1 \right)$, where l is the stack length, and GMD_{ij} is the geometric mean distance

between tape i and j. The geometric mean distance is derived from Fig. 2 of [17]:

$GMD_{ij} = \left(0.41 \frac{D_{ij}}{w} + 0.22 \right) 2w$, where w is the tape width. An alternative expression for GMD_{ij} can be

found in [18], page 322-323. The largest variation in inductance (per unit length) is between the central tape (which has the largest inductance) and the outermost tapes in the stack, and it is about 8% for a stack 12 cm long. If the same calculation is repeated for a longer stack, the mismatch gets smaller.

In order to include also the effects of twisting and winding, the inductance has been calculated with numerical methods. We have used the M'C module of the Cryosoft package. A stack of 30 tapes (4 mm wide and 0.1 mm thick), wound in one turn of 1.9 m radius, has been considered, and each tape was modelled with iso-parametric bricks. It has been found that the inductance variation is about 4%, irrespective of the twist pitch (from non-twisted down to 20 cm twist pitch). Almost all the variation in inductance comes from the summation of the mutual inductances. Therefore, at least for this case (stack of tapes in a large coil), twisting does not significantly reduce the inductance variation and thus does not homogenise the current distribution.

The first cabling stage of DEMO RW2 conductor [14], which is composed of "partially transposed" strands, has also been analysed. This first stage is composed of 18 strands (1 central copper wire + 6 Nb_3Sn strands + 12 Nb_3Sn strands) and both layers of wires have the same twist pitch of 95 mm. The variation in inductance between the strands in the inner layer and the one in the outer one is about 2%; if the twist pitch is reduced to 60 mm, the inductance variation becomes 4%; for 20 mm twist pitch, the variation in inductance is 16%.

One more conductor that has been studied is the non-twisted, non-transposed NbTi conductor used for the fabrication of the T-7 tokamak [5]. The conductor is composed of 16 large NbTi strands arranged in two rows (see Fig. 2 in [4]). The maximum variation in inductance between the strands is about 10% (winding radius is 0.5 m). All these values are summarized in Table 1.

Table 1. Estimated inductance variation in non-transposed cables

cable	Twist pitch	Max inductance variation (per meter)
stack of 30 tapes (wound on R= 1.9 m)	Infinite	4%
	1000 mm	4%
	200 mm	4%
1+6+12 Nb_3Sn (wound on R= 1.9 m)	95 mm	2%
	60 mm	4%
	20 mm	16%
T-7 (wound on R= 0.5 m)	Infinite	10%

To assess whether a value of inductance mismatch is acceptable or not from the stability point of view, one should also consider the transverse resistance between the strands, the ramp rate and the temperature margin: the idea is that current unbalance causes current redistribution, which takes place through resistive materials, thus generating heat (see [19]). Moreover, current imbalance is a source of field errors, at least during the current ramp. All these analyses should be carried out on a case-by-case basis. Nonetheless, table 1 suggests that inductances mismatches of few % (4% for the HTS stack and 2% for the 1+2+6 Nb_3Sn sub-cable) are tolerable. Even in the T-7 magnet, it was concluded that the reason why the design field was not reached was flux jump instabilities in the fully coupled conductor, rather than current unbalance.

HTS cables could probably tolerate larger inductance variations (and thus current inhomogeneity) than LTS cables because they are much more stable, see for example [20]. If the strands are insulated (i.e. exchange current only at terminals), then the inductance mismatch must be much smaller, as reviewed in [19].

4. AC loss

Currents are induced in normal and superconducting materials in presence of time-varying magnetic field. The losses associated with the induced currents can be classified according to the material in which the current flows:

1) Eddy current loss – currents flow only in normal metals. These are evident only at very high sweep rates and are not considered here.
2) Hysteretic loss – currents (also called screening or magnetisation currents) flow only in the superconducting material. Transport current losses can be neglected in magnets, because are smaller than the hysteretic loss.
3) Coupling loss – currents flow in superconducting and normal material (the current loop is closed through normal materials).

4.1 Hysteretic losses

Hysteretic losses are proportional to the width of the superconducting material, for the same current density (see [8] section 8.2 or [23]). In Nb_3Sn and NbTi multifilamentary wires the hysteretic losses are minimised by decreasing the filament diameter down to few microns. In a coated conductor tape the hysteretic loss would be much larger than in multifilamentary wires, because the width of the tape is several mm. If the tape is twisted, the loss is $2/\pi$=0.64 of the loss of the non-twisted tape, as demonstrated in [15], section 7.2.2; a similar analysis has been carried out in [20] and in [21]. The reason is that the loss in thin tapes depends only from the perpendicular component of the magnetic field; the factor $2/\pi$ is the average of the perpendicular component over a twist pitch. The term $2/\pi$ is the same order of magnitude of 1, meaning that loss reduction is modest. In coated conductor tapes the effective width is always of the order of mm, three orders of magnitude larger than in LTS.

4.2 Coupling losses

As mentioned in section 2, the coupling loss is controlled by the value of the critical twisting length $L_c = \sqrt{\dfrac{d\rho J_c}{dB/dt}}$, where d is the superconductor thickness, ρ the matrix resistivity, dB/dt the magnetic field sweep rate. As discussed in [8] and [22], when the length of the sample (in non-twisted conductors), or the twist pitch (in twisted conductors) is shorter than L_c, the coupling current is smaller than the screening current in the superconductor (the so-called uncoupled case). Coupling loss grows with the square of the twist pitch only until the twist pitch is the same order of magnitude of L_c. When the sample length or the twist pitch is comparable or longer than L_c, the coupling current has the same magnitude of the screening current in the superconductor. The filaments (or the tapes in a stack) are then fully coupled and the conductor behaves like a monolithic one with homogeneous current density. Then the coupling loss saturates to the value of hysteretic loss of the monolithic conductor, the so-called saturated (coupling) loss. Saturated losses, like hysteretic losses, do not depend on frequency; the reason is that the time constant being extremely large, there is actually no dependence from the sweep rate. Analysis of the various loss regimes is reported also in [23].

The critical twist pitch in NbTi is of the order of few tens of mm (see table 2), therefore the typical twist pitches in commercial NbTi wires is less than few tens of mm. In NbTi wires, critical current density and manufacturing costs are unaffected by twisting (even at short pitches), while large coupling losses cannot be tolerated because of the very small temperature margin.

In Bi-2223 tapes, L_c is about the same order of magnitude than in NbTi wires (see table 2). Bi-2223 tapes with twisted filaments were produced in the past, and indeed AC losses were lower than in non–

twisted tapes, but only at low frequency (<10 mT/s, typical of high field solenoids). However, the disadvantages of twisting were significantly lower current density and lower manufacturing yield (thus higher price and shorter length). In Bi-2223 tapes, low AC loss is less valuable than current density, and Bi-2223 tapes with twisted filaments are not produced anymore by Sumitomo, while non-twisted tapes are still produced and employed in magnets and cables. Low losses at higher sweep rates can be obtained in Bi-2223 tapes with twisted filaments and resistive barrier surrounding each filament. These tapes were investigated in the 90's, but were even more difficult to manufacture and never reached industrial production.

Table 2. Examples of critical twist pitch for various strands and conductors.

	NbTi strand 4 K, 5 T	Bi-2223 tape 4 K, 15 T	Stack of soldered REBCO tapes 4 K, 15 T	Stack of non soldered REBCO tapes 4 K, 15 T
Superconductor thickness	10 μm	24 μm	2 μm	2 μm
J_c	$2 \cdot 10^9$ A/m^2	$1 \cdot 10^9$ A/m^2	$4 \cdot 10^{10}$ A/m^2	$4 \cdot 10^{10}$ A/m^2
Matrix resistivity	$4 \cdot 10^{-10}$ Ωm	$2 \cdot 10^{-10}$ Ωm	$2 \cdot 10^{-8}$ Ωm	$2 \cdot 10^{-7}$ Ωm
dB/dt	0.05 T/s	0.05 T/s	0.05 T/s	0.05 T/s
L_c	34 mm	28 mm	506 mm	1600 mm

The losses in multifilamentary, non-twisted Bi-2223 tapes are the saturated losses of the monolithic conductor formed by the envelope of the filaments, and Bi-2223 magnets work fine even if the tape is operated in saturated loss regime. How would the losses of a non-twisted stack of three REBCO tapes (each 1.3 mm wide and 0.1 mm thick) compare with the one of a Bi-2223 tape? In both cases we are dealing with saturated coupling loss, which can be calculated as the loss of the corresponding monolithic conductor. We consider the loss when the conductor (a Bi-2223 tape or a non-twisted stack of three REBCO tapes) is wound in a solenoid. As described in [24-25] the loss is the sum of the loss associated to the axial field component (parallel to the broad face of the conductor) plus the loss associated to the radial field component (perpendicular to the broad face of the conductor). The infinite slab model should be used for both components. This model is applied to each tape for the axial component and to the whole pancake for the radial component, because of the magnetic interaction between conductors. In fact the conductors in the pancake interior (or in a stack) are screened from the outermost tapes (see [24-25]). In both orientations, the conductor can be treated as an infinite slab. The loss (J/m^3) for an infinite slab (cycling between –B and +B) is ([8], section 8.2.1):

$$Q = \begin{cases} \dfrac{2}{3\mu_0} \dfrac{B^3}{B_p} & B < B_p \\[2mm] \dfrac{2B_p}{\mu_0}\left(B - \dfrac{2}{3}B_p\right) & B > B_p \end{cases} \qquad (1)$$

In case of the Bi-2223 tape, for axial loss (field parallel to the wide face of the tape) $B_p = \mu_0 J_{sc}\dfrac{t}{2}$ and $J_{sc} = \dfrac{I_c}{wt}$, where t=0.18 μm is the filament region thickness and w=4 mm is the filament region width; the loss per unit length (J/m) is then $Q_z = Q \cdot w \cdot t$. For radial loss (field perpendicular to the tape),

7

$B_p = \mu_0 J_e \dfrac{w}{2}$ and $J_e = \dfrac{I_c}{wd}$, where w=4.2 mm is the tape width and d=0.30 mm is the total tape thickness including insulation; the loss per unit length (J/m) is then $Q_r = Q \cdot w \cdot d$.

In case of a non-twisted stack of three tapes (each tape 1.3 mm wide and 0.1 mm thick), for axial loss $B_p = \mu_0 J_e \dfrac{d}{2}$, where $J_e = \dfrac{I_c}{wd}$, and d =0.2 mm is the distance between the outermost ceramic layers.

For radial loss $B_p = \mu_0 J_e \dfrac{w}{2}$ and $J_e = \dfrac{I_c}{wD}$, where w=1.3 mm is the stack width and D= 0.35 is the total stack thickness including insulation.

The field dependence of the critical currents at 4.2 K for a representative Bi-2223 tape and a 4 mm wide coated conductor is plotted in Fig. 1. It should be said that equation (1) is valid only for constant current density; however the idea is to use (1) multiple times for various B and the corresponding value of current density at that B value.

When the loss per unit of critical current (J/m·A) is considered (see Fig. 2), the non-twisted stack of REBCO tapes has comparable or lower loss than the Bi-2223 tape at any magnetic field (> 1 T) and for both orientations of the magnetic field. This suggests that a non-twisted stack of few REBCO tapes could be used in any magnet that was successfully operated with Bi-2223 tapes, i.e. dipoles, MRI coils and NMR inserts.
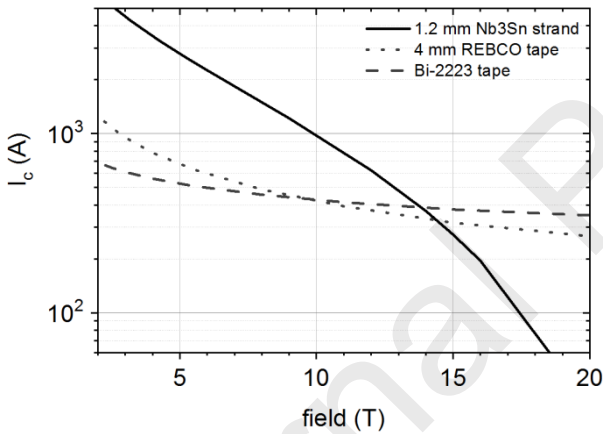

Fig. 1. Critical current versus field (at 4.2 K), for the wire and strands discussed in this paper. The curves are analytical equations representative of commercial wires and tapes.
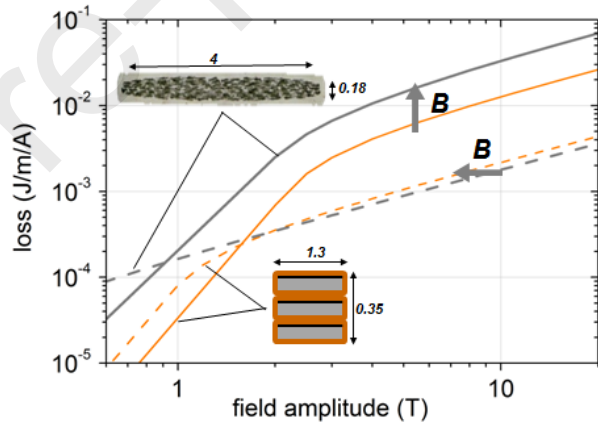
Fig. 2. Saturated loss divided by the critical current for a non-twisted stack of tapes (orange) and for a Bi-2223 tape (grey). Both parallel (dashed lines) and perpendicular (solid lines) magnetic field orientations are shown.

There is another loss reducing strategy that can be used with materials that cannot be easily twisted, as discussed by Campbell in [23]: "*using a thin conductor … in the direction perpendicular to the field*". In fact, the hysteretic loss (and the saturated coupling loss) is proportional to the width of the conductor, at fields larger than the penetration field; the width is defined as the projection of the conductor in the plane perpendicular to the field direction. It follows that by modifying the aspect ratio of the conductor, it is possible to control the loss for a given field direction.

In Fig 2 in [26] the effect of the aspect ratio on loss is shown for a rectangular conductor: the loss is basically proportional to the aspect ratio. This method is effective also in Bi-2223 tapes, i.e. adjusting the aspect ratio of the tape, from thin tape to square wire, according to the magnetic field direction, see for example [27] and the conclusion in [28].

In coated conductors, the aspect ratio can be easily varied by replacing a single tape with a stack of narrower tapes. Let's compare the loss of a the non-twisted stack of three tapes with the one of a single wide tapes. In case of a single tape, the loss is calculated again with equation (1), with $B_p = \mu_0 J_{sc} \dfrac{t}{2}$ for axial loss (field parallel to the tape), where $J_{sc} = \dfrac{I_c}{wt}$, t=1 µm is the ceramic layer thickness and w=4 mm is the tape width; the loss per unit length (J/m) is then $Q_z = Q \cdot w \cdot t$. For radial loss (field perpendicular to the tape), $B_p = \mu_0 J_e w$, where $J_e = \dfrac{I_c}{wd}$ and d=0.15 mm is the total tape thickness including insulation; the loss per unit length (J/m) is then $Q_r = Q \cdot w \cdot d$.

The saturated loss (J/m) of the non-twisted stack of three tapes is plotted in Fig. 3 together with the loss of the 4 mm wide tape. The non-twisted stack shows lower loss when the magnetic field is large (> few T) and perpendicular to the stack. At low magnetic fields and at large field parallel to the tape, the single tape has the lowest loss.
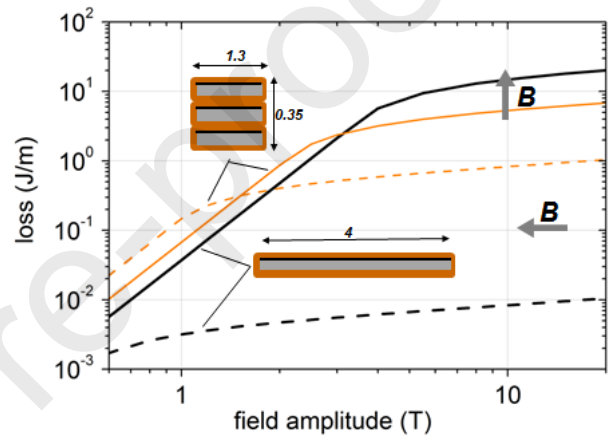

Fig. 3. Hysteretic loss (J/m) for a 4 mm wide tape (grey) and saturated loss for a non-twisted stack of three 1.3 mm wide tapes (orange). Both parallel (dashed lines) and perpendicular (solid lines) magnetic field orientations are shown.

4.3 Example of losses in twisted and non-twisted cables

In this section, the effectiveness of twisting is studied in two sub-cables: a twisted Nb$_3$Sn sub-cable and a stack of coated conductors. They follow the design of two experimental conductors: the Nb$_3$Sn sub-cable is employed in the conductor manufactured and tested by SPC for the EU-DEMO [14]; the square stack is the sub-cable of a flat conductor that is proposed also by SPC for the Central Solenoid of DEMO [29].

The limit cases considered here are the fully uncoupled (hysteretic loss only) and fully coupled (saturated losses) cases. The description of the intermediate case for twisted multistage cables is rather complex.

The Nb$_3$Sn sub-cable is composed of 12 around 6 strands (1.2 mm $\varnothing$) cabled around a central copper wire. Cu:nonCu ratio is 1 and each strand is assumed to contain 2500 filaments of 10 µm diameter. The field dependence of the strand critical current is shown in Fig. 1. If neither the strands nor the filaments are twisted (coupled filaments), the saturated loss (J/m^3) can be calculated using the expression for a cylinder in transverse field (see [8], page 165-169), where the diameter is the one of the sub-cable and the current density is calculated over the whole cross section. If both strands and filaments are twisted (uncoupled filaments), the hysteretic loss is calculated with the same formula,

but now the diameter is the filament diameter and the current density is the one in the filaments. This is an approximation, because the strand layers in fig. 4 are not transposed. In case of sufficiently low sweep rate, short twist pitch and high transverse resistance, the coupling losses are negligible, and the hysteretic loss is the only loss contribution. The losses for the two cases are plotted in Fig. 4: the benefit of twisting fine filaments and strands is an evident reduction of almost two orders of magnitudes in losses at large field amplitude. In other words, filament hysteretic losses are much smaller than the saturated loss.

The stack of coated conductors is composed of 30 tapes, each 3.3 mm wide, resulting in a square stack; the field dependence of I_c for one tape is shown in Fig. 1. The saturated loss (J/m³) for the non-twisted stack can be calculated from χ'', the imaginary part of the complex susceptibility, as described in [40]: $Q = \pi\mu_0 H^2 \dfrac{\chi''}{\chi_0}\chi_0$, where χ_0 is equation (13) in [30]. The χ''/χ_0 values as a function of $h = H/H_p$ can be found in table 2 in [30] for rectangular conductors of various aspect ratio. $H_p = \dfrac{J_e b}{\pi}\left[\dfrac{2a}{b}\arctan\dfrac{b}{a} + \ln\left(1 + \dfrac{a^2}{b^2}\right)\right]$ is the penetration field for a rectangular conductor, where a is the stack half width and b is the stack half height, here $a=b=1.65$ mm; $J_e = \dfrac{I_c}{2a \cdot 2b}$. The saturated loss (J/m) is obtained by dividing Q by the stack cross section and is plotted in Fig. 4 (dashed green line). If the stack is twisted, the loss is only $2/\pi \sim 0.64$ of the loss of the non-twisted stack, as is the case of a single tape. In other words, the hysteretic loss of a twisted stack is almost as large as the saturated loss of a non-twisted stack.

Large hysteretic losses in stack of tapes have been confirmed experimentally. The magnetisation loop of a non-twisted stack (28 tapes, 3 mm wide) was measured at Frascati (see Fig. 9 in [31]): from the area of the magnetization loop (full cycle of 12 T amplitude) the hysteretic loss can be estimated to be about 260 J/m, which agrees with Fig. 4. The corresponding energy loss density would be about 35000 kJ/m³ (8700 kJ/m³ for a field ramp from 0 to 12 T). The magnetization loop was also measured at an angle of 45° between the stack and the magnetic field (see Fig.11 in [31]). The loop area, and thus the loss, is just slightly lower than the one for the field orientation perpendicular to the tapes; the losses vanishes only when the field is parallel to the tapes. These measurements prove that hysteretic losses in twisted stacks are only marginally lower than in non-twisted ones.
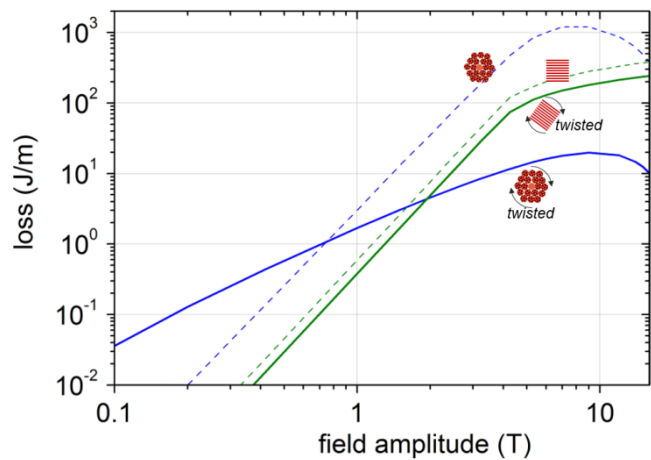

Fig. 4. Hysteretic loss (twisted, solid lines) and saturated coupling loss (non-twisted, dashed lines) for the stack of tapes (green) and the Nb_3Sn sub-cable (blue).

To summarise, twisting is very effective in reducing total losses only if the twist pitch is much shorter than L_c and if the filament diameter is much smaller than wire diameter. For example, in multifilamentary LTS strands and cables, twisting (i.e. magnetically decoupling) round, fine filaments, the effective diameter drops from few millimetres to few microns (two or three orders of magnitude smaller). Instead, twisting a stack of tapes is a very ineffective loss reduction strategy (less than 36% reduction), because the effective width decreases only marginally. If coated conductor tapes could be subdivided into very narrow (few tens of micron) filaments, the so-called striation process, the loss of a twisted stack could be drastically lower than the one of a non-twisted stack (see for example [26]). The above considerations on losses will be applied to various types of magnets in the next sections, growing in size and complexity, from high field solenoid and dipole (section 5.2) built with few tapes to large conductors for fusion magnets (section 6).

5. Loss in high field solenoids and dipoles

5.1 Loss in small high-field solenoids

Even if a large number of coils and magnets have been built with coated conductors in the last decade, there are few publications dealing with analysis and/or measurement of ramping loss. A relatively well-studied case is the cryogen-free 25 T magnet at Tohoku University: the magnet consists of a LTS outsert (wound with NbTi and Nb_3Sn Rutherford cables) and an HTS insert, which is wound with a 5 mm wide coated conductor; see [32] for the characteristics of the coils. This section reviews the results published in [24] and [25], adding minor observations.

In the HTS insert the main loss component is the hysteretic one. The hysteretic loss can be estimated [24-25] as the sum of the loss associated to the axial field component (parallel to the broad face of the tape) plus the loss associated to the radial field component (perpendicular to the broad face of the tape). The infinite slab model is used for both components. In [24-25] the instantaneous loss was calculated and formula (6) in [24] is simply the time derivative of the well-known formula for an infinite slab, see also [8], pag. 162-163. An additional term accounts for the loss due to transport current (see also [23], page 10-11), but this term is less than 1% for the axial component and <10% for the radial component; therefore it could be neglected for rough estimations.

It was found (see Fig. 6b in [24]) that at the beginning of the field ramp (<5 T) the largest loss contribution originates from the axial field. The reason is that the penetration field is only few tenths of tesla for the tape oriented parallel to the field. Later during the field ramp, at larger fields (>10 T), the largest contribution to the instantaneous loss comes from the coil volume exposed to large radial components of the magnetic field. The reason is that for pancakes at coil ends the penetration field is several tesla, and the loss (J/m) keeps growing with the square of field (formula (6) in [24]) up to the penetration field.

In [33], the AC loss during ramp from zero to the peak field was estimated at 6.5 W in the HTS insert and at 2.6 W in the LTS coil. The HTS coil volume can be evaluated from the coil dimensions [32] to about 0.021 m^3, while the LTS coil volume is about 0.20 m^3. Then the peak instantaneous losses per unit volume are about 315 W/m^3 for the HTS insert and 13 W/m^3 for the LTS outsert. It should be stressed that these are average values over the whole volume of the coil. The loss density at the HTS coil ends is much larger; for example, the peak instantaneous loss is about 1800 W/m^3 (0.5 W from Fig.5 in [25] divided by the volume of one pancake) in the outermost pancakes. In terms of energy density deposited during the charging ramp, the loss in the whole HTS coil is about 850 kJ/m^3. In the top pancake it would reach over 2700 kJ/m^3; this value is comparable (order of magnitude) to the ones of twisted and non-twisted stacks of REBCO tape, as reported in section 4.3.

One more striking difference between the LTS and the HTS coils regards the evolution of the power loss during the ramp. In the LTS, the instantaneous power loss is mainly due to coupling loss, which is constant during the whole ramp (constant ramp rate). On the contrary, in the HTS coil, the instantaneous power loss is hysteretic; it is proportional to B^2 when $B<B_p$, then decreases with $J_c(B)$ for $B>B_p$. In the case of the pancakes, the penetration field is several tesla: the radial component of the magnetic field will exceed this value only at the end pancakes, while in the pancakes around the coil mid-plane, $B<B_p$ during the whole ramp. It follows that in the whole coil, the total power loss grows till the end of the ramp (see fig. 6 in [24]); the maximum value is reached at the end of the ramp, when the field is the highest and the critical current and temperature margin are the lowest.

The analysis of losses is in agreement with the measurements of the temperature of the coils, as shown in [24] and [33]. The temperature of the HTS coil raised from 4.3 K to about 7.6 K during the energization of the magnet; in contrast, the temperature of the LTS coils increased only to 5.1 K. The HTS coil could be operated at such high temperature because HTS magnets have a much larger temperature margin than any LTS magnets. It is important to stress that the cooling capacity does not need to be increased to face the larger heat load. In fact, as discussed in [33], the cooling efficiency of GM cryocoolers rises with temperature: when the operating temperature is raised from 4.2 K to 8 K, the cooling capacity increases from 1.5 W to 10 W, for the same electric power consumption at room temperature. The modification to the cooling system simply consisted in using two different cooling circuits for the LTS and HTS magnets, so that the two coils can be operated at different temperatures. A similar analysis was published in [34] by the Chinese Academy of Sciences, in Beijing. The magnet is a split coil wound with Bi-2223 tapes. In the Bi-2223 split coil the energy loss per unit volume is about 750 kJ/m^3.

The ramping loss of the 17 T HTS insert at NHFML has been calculated with finite element methods [35]: the loss per unit volume is about 1000 kJ/m^3.

5.2 Loss reduction - Stack of non-twisted tapes for solenoids and dipoles

Ramping loss in HTS tape coils is at least one or two orders of magnitudes larger than in LTS multifilamentary coils, but the enormous amount of heat does not prevent the operation. A more important effect, at least for some applications, is the perturbation of the central field caused by the magnetisation. In HTS solenoids, the largest contribution to the loss comes from the field component perpendicular to the tape at the coil ends. According to the discussion of section 4.3, the residual magnetization (and losses) in solenoids and dipoles could be reduced by changing the aspect ratio of the tape at the coil ends, where the radial field component is larger. In long coils (for example NMR coils), where a large volume is exposed to axial field, the non-twisted stack may not provide the lowest magnetisation, if used in the whole coil volume. But in short coils (for example dipoles, or insert for laboratory magnets), it may be advantageous (lower magnetisation) to replace a wide tape with a stack composed of few, narrow tapes. This would naturally lead to axial grading, and applications to solenoids and dipoles are briefly discussed. In stand-alone coils wound with coated conductors, axial grading of the critical current (wider tape at the coils ends) is beneficial, because it allows generating the same field with less material than in a non-graded coil (see for example [36]). The graded magnet in [36] was wound with 4.1 mm tapes in the mid-plane pancakes, and with tape of increased width up to 8.1 mm in the pancakes at the magnet's ends. The disadvantages of using wide tapes at the magnet's ends are large magnetization field and large loss. Both disadvantages can be eliminated by replacing the wide tape with a stack of narrow tapes (for example 3 tapes each 3 mm wide), as schematically shown in Fig. 5 left.

12

The CEA block coil dipole [37] is also wound with a stack of two non-twisted tapes (each 12 mm wide). The coil is composed of a central double pancake and two smaller pancakes on top and bottom, all wound with a two-in-hand conductor. The conductor is composed of two 12 mm wide tapes soldered to a central copper tape and sandwiched between two CuBe tapes (see Fig. 3 in [34]). In this coil the screening currents perturbed the magnetic field in the dipole centre [38]. The magnetization could be reduced by replacing the top and bottom pancakes with pancakes wound with stack of few, narrow tapes, for example 3x8 mm and 6x4 mm. This configuration is schematically shown in Fig. 5 right.

Also regarding dipoles, Roebel cables have been considered for the construction of high field dipoles (see a review in [3], section 4.1). Tapes in Roebel cables are uncoupled only when the field is parallel to the wide face of the tapes [39], instead, for perpendicular fields, the tapes are fully coupled. Therefore, a Roebel cable would have lower loss and lower magnetization than a non-twisted stack only in magnet sections where the field is mainly parallel to the tapes.

Regarding coil manufacturing, non-twisted stacks of few tapes (2 to 5) can not be assembled as a cable to wind magnets (small diameter), because the tapes are not length-compensated. Therefore, all the tapes should be co-wound; this technique is seldom used and would need extensive development.
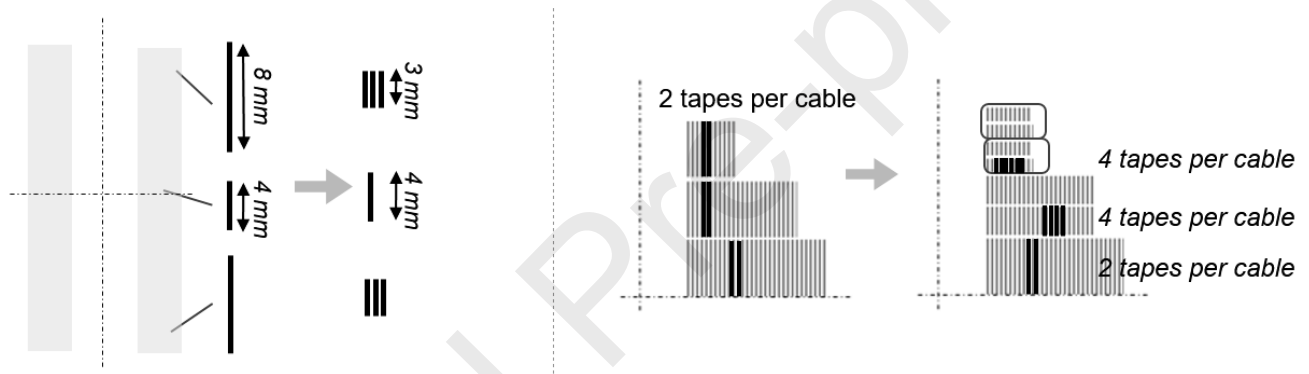

Fig. 5 Schematic illustration of the proposed replacement of wide tapes with non-twisted stacks of narrower tapes. Left: graded solenoid, based on [36]. Right: dipole, based on the CEA dipole [37].

A recent experiment [40] from the Shanghai University has demonstrated the reduction in magnetisation. Two coils with similar dimensions were prepared: one was wound with a single 5 mm wide tape, the other with a stack of two 1.5 mm wide tapes. The magnetization in the coil centre was found to be larger for the 5 mm tape coil than the one of the 2x1.5 mm tape coil.

A much older example [42], is a small coil (13 mm inner diameter, 140 mm outer diameter, 82 mm height) wound with a non-twisted stack of 3 monofilamentary Bi-2212 tapes. The ramping loss to 0.4 T (the coil was operated at 20 K) was estimated from the temperature increase to about 16 kJ/m^3.

Only the Brookhaven Technology Group Inc. has dared to fabricate non-twisted stacks of more than two tapes [41]: their ExoCable™ is composed of a stack of exfoliated ceramic layers, each with the corresponding copper layer. A 10 m long cable was manufactured by assembling and soldering together a stack of eight exfoliated tapes (each 2.4 mm wide), resulting in a 1.2 mm thick conductor. The remnant magnetisation in the coil wound with such cable was lower than that of a coil wound with a 12 mm wide tape (see Fig. 14 in [41]). The measured hysteresis curves have been modelled considering the cable as a rectangular slab. This confirms that the ceramic layers are fully coupled and behave like a monolithic conductor, and that the method used to obtain Fig. 2 and 3 is valid. The rectangular slab model will be used to describe losses in thicker stacks in section 6.

For both the Shanghai University and Brookhaven Technology Group experiments, the magnetisation is proportional to the stack width, but for thicker stacks made of narrower tape, the effect of the field generated from saturated coupling current may not be negligible anymore.

5.3 LTS tape magnets

What would have happen if a coil like the HTS insert of Tohoku University had been built with LTS coated conductor? This may seem a strange question today, but Nb_3Sn ribbons (12 mm wide, substrate <50 micron) have been available commercially from four different producers during the 60's and 70's, and several magnets were built with such ribbons. It has been reported [43] that those magnets often quenched at fields much lower than the one expected from the performance of short sample. The explanation was flux jumping, because LTS tapes are prone to flux jump instabilities when exposed to perpendicular fields of 1 T or less. The solution was to add very thick stabilizing layer (for example very high purity aluminium), but better cooling was found to be more effective [44]. According to the examples in section 5.1, ramping losses of Nb_3Sn ribbon magnets would be about two order of magnitude larger than in Nb_3Sn multifilamentary magnets: perhaps the reported instabilities were not entirely due to flux jump, but also favoured from the large ramping loss which further reduced the temperature margin.

6 Cables for fusion magnets

Magnets for fusion and for large detectors have operating currents exceeding 20 kA; this implies that hundreds of tapes must be assembled in a cable. Because of the very large number of tapes, the cable usually consists of sub-elements. The sub-elements considered so far are the tapes stack, the CORC and the Roebel cable; an overview of the present research activities is available in [3], sections 4 and 5. In the last few years, the most studied sub-element is the stack, which was first introduced by MIT [15].

Before evaluating the loss in cables, values of field sweep amplitudes (ΔB) and sweep rates are introduced. The values here and in the following sections are from DEMO EUROfusion (2015 version), are only indicative and to be used as example for loss assessment. In large tokamaks, the Toroidal Field (TF) magnets will be ramped at sweep rates between 0.001 and 0.01 T/s; the field sweep (ΔB) is about 12 T (up to 20 T for compact, HTS tokamaks). This range of sweep rate is the same of small laboratory magnet, NMR, and even the LHC dipoles. Instead, the Central Solenoid (CS) operation is characterised by different amplitudes and rates, see for example [45]. The field is usually swept from about -12 T to 12 T, but with the use of HTS, fields up to 17 T have been considered. Assuming a 16 T CS field, as in [40], the three most demanding CS operation modes, regarding AC losses, are:

- Dwell phase: field sweeps from -16 T to 16 T; sweep rate between 0.05 and 0.1 T/s.
- Breakdown phase: ΔB is almost 1 T at peak field (16 T); sweep rate is at least 1 T/s.
- Plasma current ramp-up (PCRU) phase: field sweeps from 15 T to about 0 T; sweep rate between 0.2 and 0.3 T/s.

Large fusion conductors are tested over a broad range of sweep rates but at small AC field amplitude (<0.5 T), for example at Twente University or in EDIPO/SULTAN at SPC. In the EDIPO/SULTAN facility, the static background field is up to 10 T, with a maximum AC field amplitude of 0.4 T; the sweep rate can vary from about 0.1 T/s to about 3 T/s, roughly corresponding to frequencies between 0.1 and 3 Hz.

6.1 AC loss in large cables composed of twisted tape stacks

Losses on an HTS experimental cable composed of twisted stacks have been measured in EDIPO [46], following the same procedure and in the same conditions of ITER conductors. These measurements showed that hysteretic losses were negligible and that the coupling losses were moderately larger than in Nb_3Sn CICC. This result is not valid over the whole range of field amplitudes and sweep rates of interest for the CS operation, as explained below.

The power coupling loss can be described with $P_{cp} = \dfrac{n\tau}{\mu_0} S \dfrac{dB^2}{dt}$, with $n\tau$=0.075 s and S=0.0007 m^2 [45].

These parameters are valid for the the LTS multifilamentary cables and for the HTS cable. In fact, in [29] it has been estimated that an HTS conductor composed of 12 square stacks (see fig. 6) would have similar coupling loss that a flat Nb_3Sn multifilamentary cable. The same coupling power loss in the HTS and LTS conductor have been retained also by EUROfusion and used for the estimation of the temperature margin in [45].

The hysteretic loss in the HTS cable can be estimated calculating the energy loss for a square conductor, as described in section 4.3; for a twisted stack, the loss should be multiplied by 0.64. The values obtained from this procedure are confirmed by magnetization measurement at ENEA on a stack of tapes. In fact, the loss can be estimated from the magnetisation loop (Fig. 9 in [31], full cycle from –B to +B) at about 260 J/m for one non-twisted stack, corresponding to about 160 J/m for a twisted one. This is in agreement with Fig. 4, where the hysteretic loss for a twisted stack is about 200 J/m for 12 T field amplitude. The hysteretic power loss is then calculated as the time derivative of the energy loss.

The coupling and hysteretic power losses (ramping from 0 to B) are plotted in fig. 6 as a function of field for three sweep rates. Coupling power losses are constant with the field; at fixed amplitude, they grow with the square of the sweep rate. Instead, hysteretic power loss grows with the square of the field (up to penetration field), then slowly decrease with the field dependence of the critical current. A similar behaviour is observed also in magnets built with single tape (see for example Fig. 6 in [24]). At fixed field, hysteretic power loss is linear with the sweep rate.

In the region accessible by the EDIPO/SULTAN test setup (0–0.4 T, 0–1 T/s), coupling power loss is larger than hysteretic loss. However, at larger field amplitude, the hysteretic loss becomes the largest contribution even at 1 T/s; only at much larger sweep rates the coupling loss is the largest one for every B. This is a specific feature of tape conductors. In fact, in case of fine multifilamentary conductors, the hysteretic losses would be lower than the coupling loss over almost the whole range of field and sweep rates shown in fig. 6.

In [2], it is claimed that coupling loss is the main loss contribution in HTS stack cables; this statement is inaccurate, because its validity is limited to field amplitudes smaller than the penetration field of the stack. At such fields (< 0.4 T) most of the stack is screened from the magnetic field, and the losses originates only from few tapes located on the stack exterior. Instead, when the ΔB exceeds few tesla (full penetration), the main source of loss in tape stack cables will be the hysteretic one.

The coupling and hysteretic losses for the four CS operating cases are reported in Table 3. The hysteretic loss during breakdown is calculated with 1 T AC field amplitude, using the current density at 15 T instead of 1 T. Another consequence of fig. 6 and Table 3 is that the thermo-hydraulic analysis in [45] underestimates the temperature increment, because it takes into account only coupling loss and neglects the contribution from the hysteretic loss, which is the largest one during the plasma current ramp-up and dwell phases. For example, the loss in [45] during the dwell phase was 0.1 W/m, while the peak power hysteretic loss would reach a value orders of magnitude larger (see fig. 7).

15

In conclusion, ramping losses in large HTS cables (composed of twisted stacks) are much higher than in LTS multifilamentary cables, because of the large hysteretic losses in tapes. It is the same reason why ramping losses in small HTS solenoids are orders of magnitude higher than in LTS solenoids (see section 5.1).
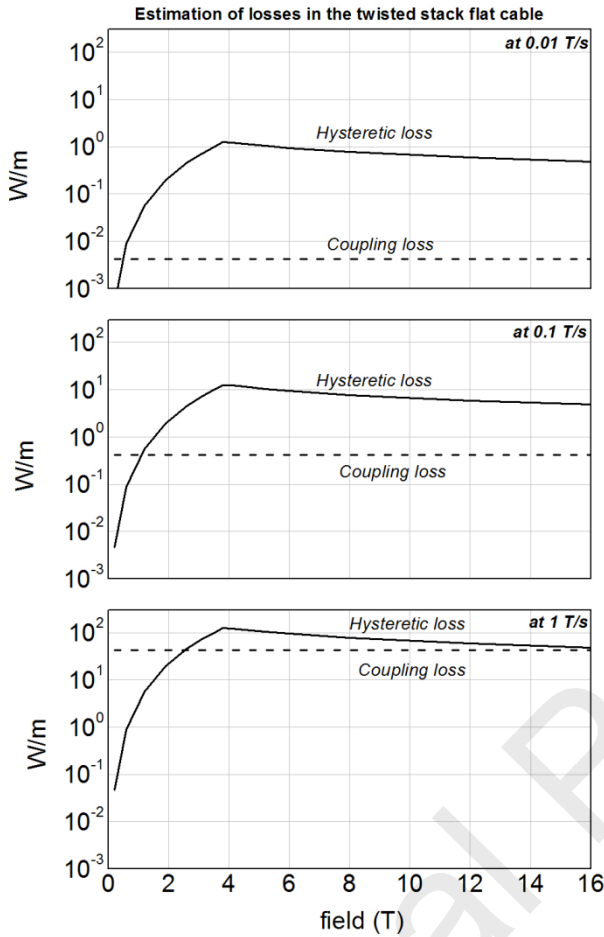

Fig. 6. Coupling power loss (dash line) and hysteretic power loss (solid line) for the HTS twisted stack cable for three different sweep rates.
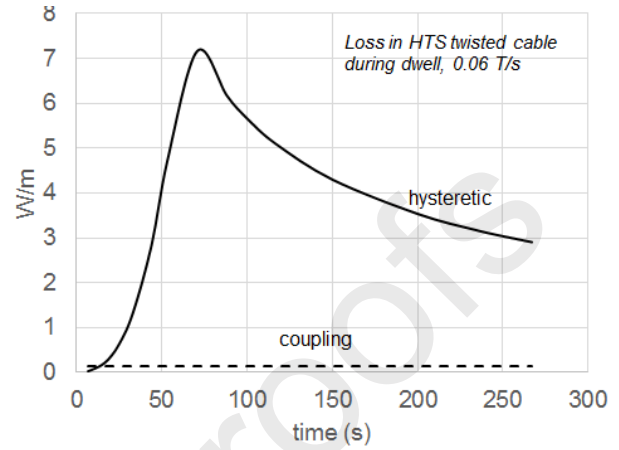

Fig. 7. Coupling power loss (dash line) and hysteretic power loss (solid line) during a sweep rate from 0 to 16 T at 0.2 T/s (second half of the dwell phase).

Table 3. Loss estimation for the HTS twisted stack flat cable in the Central Solenoid.

	Dwell	Breakdown	PCRU	burn
ΔB	-16 T to 16 T	16 T to 15.2 T	15.2 T to -2.5 T	-2.5 T to -16 T
Sweep rate	0.055 T/s	1 T/s	0.22 T/s	0.002 T/s
duration	600 s	0.8 s	80 s	7200 s
Hysteretic loss	1300 J/m	42 J/m	660 J/m	540 J/m
Coupling loss	72 J/m	33 J/m	150 J/m	1.2 J/m

6.2 Twisted and non-twisted conductors for fusion magnets

Once it is acknowledged that twisted stack conductors have intrinsically very large losses, one could evaluate losses in cables composed of non-twisted stacks, varying the dimension and aspect ratio of the stacks. In this section, this strategy will be applied to conductors for CS and TF magnets for large tokamaks.

6.2.1 CS magnets – AC loss in twisted and non-twisted conductors

The EU-DEMO (2015 version) CS is composed of five solenoid modules (from top to bottom: CSU3, CSU2, CS1, CSL2 and CSL3). The modules are powered independently, but the field is raised and decreased in all modules almost at the same time (see [47]). It follows that, at high magnetic field, the field direction in the three central modules is almost parallel to the solenoid axis (<5° misalignment). Therefore, for any magnetic field, the critical current of a tape oriented parallel to the solenoid axis is at least two times higher than the one of a twisted tape.

One option considered at SPC for the central solenoid is a flat HTS cable composed of twisted square stacks (3.3 mm x 3.3 mm), as shown in fig. 8 (see also Fig. 7 in [29]). In the three central modules (CS1, CSU2, CSL2) the number of tapes can be reduced by 50%, because the critical current is at least twice than for the twisted stack, as discussed above. Two possible ways to arrange the tapes, maintaining the parallelism with the coil axis, are the following: 1) Twelve rectangular stacks (aspect ratio is two) arranged in a Robel bar, each stack is non-twisted and contains half the number of tapes than the twisted stack cable, as shown in Fig. 8, middle bottom; 2) Assembling all the tapes in a single monolithic non-twisted stack, 26 mm wide and 2.6 mm thick, see Fig. 8, right bottom.

The hysteretic loss of the flat cable and the saturated loss of the Roebel can be estimated by multiplying the respective stack loss by 12. This procedure does not take into account the magnetic interaction between neighbouring strands, which is important at field lower than the penetration field of one stack. In fact, a superconductor shields the magnetic field not only in its interior, but also in the surrounding space. At low magnetic fields (much lower than the penetration field), the shielding ability of the stack is large. It follows that also the space in between the stacks is shielded, and the stacks behave almost like a large monolithic stack. See [48] for a more detailed discussion.

The flat cable and the Roebel cable would have the same twist pitch; therefore, the coupling losses are also similar, but are not considered here, because their contribution to the total loss is modest. In the monolithic stack, the only loss contribution is the saturated loss and it is calculated using the susceptibility for rectangular conductors [30].

The losses due to radial fields (<1 T), i.e. perpendicular to the wide face of the conductors, are several orders of magnitude smaller than the ones due to the axial field (parallel to the wide face), and can be neglected for all conductors. The axial field losses are shown in Fig. 9. The Roebel cable has lower losses than the twisted stack cable at any field amplitude; the loss of the monolithic stack are comparable to the one of the twisted stack cable at large field amplitude. Therefore, non-twisted stack conductors similar to these ones should not pose any issue from point of view of losses in the central modules of a CS magnet.
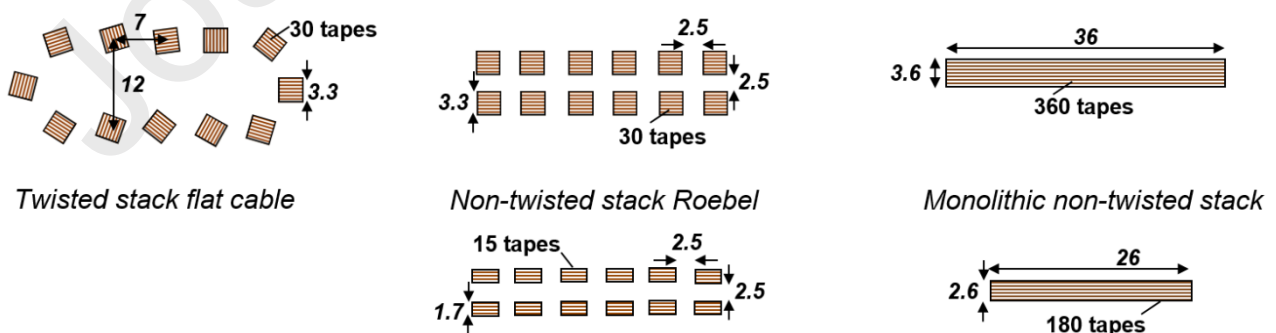

Fig. 8. Sketches of the three types of cables: twisted stack flat cable, non-twisted stack Roebel and (non-twisted) monolithic stack. Copper for quench protection, space for coolant and jacket are omitted for clarity. Stack separations are not used for AC loss estimation.

In the top and bottom modules (CSU3 and CSL3), the number of tapes cannot be reduced because the radial component is > 5 T. Therefore, the Roebel cable and the monolithic stack should now contain the same number of tapes than the twisted stack flat cable, as shown in Fig. 8 (top middle and top right). The saturated losses are now calculated with the new stack dimensions and engineering current densities and are plotted in Fig. 10 for both axial and radial field components; the maximum field ranges are indicated by the grey regions. The Roebel cable has 30% higher hysteretic losses than the twisted stack cable in both orientations. Eventually this extra power may be removed with the same electrical power if the operating temperature is increased. This disadvantage should be weighed against the advantages, for example much higher tolerance against transverse pressure. The monolithic stack has clearly much higher hysteretic losses than the other cables, because the loss due to the radial field is about 10 times larger. Of course, losses can be reduced by reducing the aspect ratio, but the minimum bending strain would increase.

6.2.2 TF magnets – AC loss in twisted and non-twisted conductors

In EUROfusion DEMO (2015 version), the peak field on the TF winding pack should be <14 T, within reach of Nb_3Sn conductors. Nevertheless, HTS cables are also investigated; one of the motivations is that, if the price of coated conductors decreases drastically in future (about an order of magnitude), coated conductors will be cheaper than Nb_3Sn even at peak fields of 12 T. The TF magnet can be slowly charged (sweep rate <0.01 T/s), but it will be subjected to the stray field of the CS and PF magnet. Nevertheless, the CS stray field component normal to the TF conductor is about 300 times smaller than the central field of the CS; therefore the sweep rate during breakdown (1 T/s in CS centre) will be <0.005 T/s (comparable to the charging field rate), and the related loss can be neglected. The PF stray field could be as high as 1 T, but the sweep rate is not yet known.

In the case of the TF magnet, the alignment of the tapes with the magnetic field is difficult to obtain, because the magnetic field is parallel (<5°) to the winding pack only in less than half of winding pack cross section. Therefore, the number of tapes should be the same as in the twisted stack flat cable. For the estimation of the loss, the data plotted in Fig. 10 should be used, the dark grey regions indicating the field of interest have been adapted to the TF. As it was the case for the CS top and bottom modules, the non-twisted stack Roebel has always 30% higher hysteretic losses than in the one of the twisted stack flat cable. The loss of the monolithic stack can be 5 times higher than in the twisted stack flat cable in some locations of the winding pack; when the losses over the whole winding pack are summed up, the total loss is two times higher than the one of the twisted stack flat cable.

During TF magnet charging, there is no nuclear heat load, therefore the extra cooling capacity could be instead used to remove the larger hysteretic losses. Thermo-hydraulic analysis should be carried out to quantify the disadvantage of large losses (from 30% to 2 times higher). The main potential advantage of non-twisted configurations is that they will likely have better tolerance against transverse pressure.
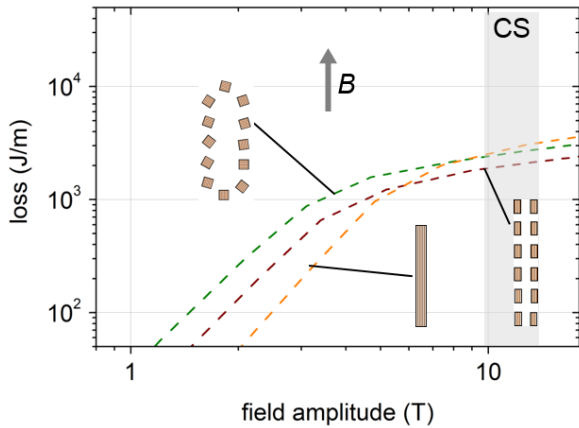
Fig. 9. Hysteretic and saturated losses in the central CS modules for the three cables. Magnetic field parallel to the wide face of the cable (axial field losses). The grey band indicate the maximum range of field in CS magnets.
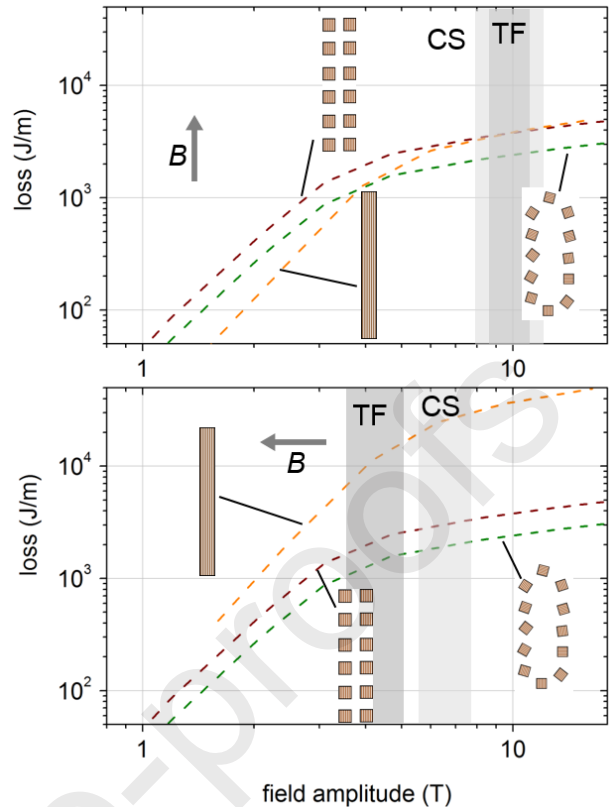

Fig. 10. Hysteretic and saturated losses in the outermost CS modules for the three cables. Top: Magnetic field parallel to the wide face of the cable (axial field losses). Bottom: magnetic field perpendicular to the wide face of the cable (radial field losses). The grey band indicate the maximum range of field in CS (light grey) and TF (dark grey) magnets.

6.3 STAR: a non-twisted conductor for helical fusion reactors

The monolithic conductor introduced in the previous section is not a new concept, because it was studied, and prototypes manufactured and tested, by the National Institute for Fusion Science (NIFS) in Japan. This conductor was developed for a large helical fusion reactor. According to the NIFS design [49], hundreds of tapes are arranged in a single stack to form a short conductor (few tens of meters). These short pieces are assembled in coil segments (each one as long as the conductors). Then the coil segments are joined together to form the full coil. The main motivation behind this procedure is to simplify the coil manufacturing. In fact, winding a large helical magnet with long pieces of conductor (about 1 km) is considered a very challenging task from the technical and industrial point of view. Instead, it is assumed that a segmented coil would be easier and cheaper to manufacture. The operating temperature should be at least 20 K, in order to remove the heat generated in thousands of resistive joints.

The effect of inductance mismatch was not assessed, but, according to NIFS, the current could redistribute at the joints. Regarding ramping loss, the hysteretic (saturated coupling) loss has been estimated in [50]: the conductor has a cross section of 3.2 mm x 3.2 mm and a critical current of 128 kA at 13 T, 25 K. The energy deposited in the conductor has been estimated to be about 4800 kJ/m^3 during a ramp from 0 to 13 T. This value is in the same order of magnitude of the non-twisted conductors discussed in section 6.2.2, and of the twisted stack conductor proposed by SPC. The ramping loss for the newest proposed STAR conductor will be likely lower by a factor 2 or 3, because it has a rectangular cross section with aspect ratio of about six, instead of a square cross section.

19

NIFS considers that the large ramping loss is acceptable because helical fusion reactor will be operated in steady state, therefore the magnet is seldom charged (it can be called "DC magnet"). This operation is similar to the operation of the TF magnet in a tokamak. Instead, tokamak CS magnets are continuously ramped during the whole power plant lifetime, and are thus considered "AC magnets".

6.4 Application and manufacturing remarks

In high field compact tokamaks, considered by Commonwealth Fusion Systems [51] and Tokamak Energy [52], the peak field would exceed 20 T at 20 K, and the whole winding pack contains only coated conductors. The high operating temperature mitigates the eventual disadvantage of non-twisted designs (large loss). At the same time, the advantages (higher current density and higher strength against transverse load) gain importance because of the high operating magnetic field and temperature. It seems plausible that the use of non-twisted stacks in these tokamaks could have much bigger impact than in the very large, low-field magnets of EUROfusion DEMO.

Regarding manufacturing and strain assessment, the monolithic conductor would behave like a solid block (the so-called "fully bonded model"), as the high friction among the tapes prevent relative movements. This cable is therefore not "length compensated", as is the case also of twisted soldered stacks. If the monolithic stack is produced in long lengths, the outermost tapes will always be in tension, while the innermost in compression during coil winding. Therefore, the tapes should be tightly packed in the conductor, to avoid lateral movements (buckling) during handling, winding and energisation. All aspects regarding manufacturing, handling and winding of non-twisted stack cables should be carefully investigated.

7. Conclusions

We have investigated stability, inductance mismatch and AC losses in twisted and non-twisted stacks of coated conductors. LTS wires must be composed of fine filaments to avoid instabilities. Instead, HTS wires and tapes can be composed of monofilaments or non-twisted filaments because HTS are much more stable than LTS.

Numerical calculations have shown that twisting a stack of tapes has negligible effect on the inductance variation among the tapes (few % for a large coil), because the mismatch originates mainly from mutual inductances. Even twisted filaments in LTS strands do not have the same inductance. These results suggest that in relatively compact conductors (few to tens mm in cross section size), transposition (zero inductance variation among the elements) or twisting are not required.

High-field magnets are usually built with a single HTS tape. These magnets have intrinsically much higher ramping losses than the ones built with fine multifilamentary wires, but they can be operated even if the instantaneous power losses are high, because of the large stability margin of HTS. If the tape is replaced by a stack of few, narrower tapes at the coil ends (for example 3 tapes, each 3 mm wide, instead of a single 12 mm wide tape), the field disturbance from screening currents (and losses) can be reduced. This is valid for solenoids and for dipoles. We have demonstrated by analytical analysis that a non-twisted stack of three, narrow (3 mm) REBCO tapes have losses comparable to a Bi-2223 tape, and can therefore be used to wind any kind of magnets that has been wound in the past with Bi-2223 tapes. Various published experiments confirm these outcomes.

In twisted cables composed of fine multifilamentary wires, the hysteretic loss is several orders of magnitudes lower than the saturated loss of the corresponding non-twisted wire/cable; coupling losses are often the main loss contribution. Instead, the hysteretic loss of a twisted stack of tapes is only marginally lower (36%) than the saturated loss of a non-twisted stack. Therefore, twisting a tape

20

stack is a very inefficient loss reduction strategy. Losses in both twisted and non-twisted stack cables can reach thousands of kJ/m^3, if the field amplitude is several Tesla (larger than the penetration field). These large losses originates from the large aspect ratio of the tapes; modifying the aspect ratio of non-twisted stacks can reduce losses. To correctly measure the loss in twisted or non-twisted stacks, applied AC fields should be larger than the penetration field of the stack (several Tesla), as is the case during the most of the operating conditions. At field amplitudes smaller than the penetration field, most of the stack interior is screened and losses are much smaller than in operating conditions.

These findings indicate that twisting stacks of HTS tapes could be superfluous, because stability, inductance and AC losses are only marginally affected by twisting. This conclusion challenges several present design concepts, but is not in contrast with the classical LTS designs, because is a consequence of stability and critical state model applied to HTS. Non-twisted stack of tapes could be used to wind a variety of magnets, from small, high field solenoids and dipoles (for example with stacks composed of 2 to 5 tapes) to large magnets for detectors and fusion (tens to hundreds of tapes). Some potential advantages of non-twisted stack designs are higher tolerance to transverse stresses and increment in critical current density. A disadvantage of non-twisted stack concepts is that winding techniques should be developed and would require modifications of present winding infrastructures.

A more general conclusion is that copying any LTS magnet technique and characteristic in HTS magnets may lead to ineffective solutions, because HTS are radically different from LTS: for example much larger temperature margin and highly anisotropic transport and mechanical properties. HTS magnets should be designed considering the specific characteristics of HTS materials and design choices should be rigorously motivated by physical analysis, not simply copied from past LTS cables and conductors.

References

[1] Fietz W. H. et al, 2016, High-Current HTS Cables: Status and Actual Development, IEEE Trans. on Appl. Supercond. 26 4800705 https://doi.org/10.1109/TASC.2016.2517319

[2] Bruzzone P. et al., 2018, High temperature superconductors for fusion magnets, Nucl. Fusion 58 103001 https://doi.org/10.1088/1741-4326/aad835

[3] Uglietti D., 2019, A review of commercial high temperature superconducting materials for large magnets: from wires and tapes to cables and conductors, Supercond. Sci. Technol. 32 053001 https://doi.org/10.1088/1361-6668/ab06a2

[4] Bruzzone P, 2006, 30 Years of Conductors for Fusion: A Summary and Perspectives, IEEE Trans. on Appl. Supercond. 16 839-44 https://doi.org/10.1109/TASC.2006.873342

[5] Ivanov D. P. et al, 1977, Test results of Tokamak T-7 superconducting magnet system, IEEE Trans. on Magn. 13 694 https://doi.org/10.1109/TMAG.1977.1059319

[6] Malkov M. P. et al, 1975, Soviet research in cryogenic technology and applied superconductivity, Cryogenics 15 65-68 https://doi.org/10.1016/0011-2275(75)90055-7

[7] Efferson K. R. et al, 1971, The IMP Superconducting Coil System, IEEE Trans. on Nuclear Science 18 265-272 https://doi.org/10.1109/TNS.1971.4326352

[8] Wilson M. N., 1983, Superconducting Magnets (Oxford: Oxford University Press)

[9] Wesche R., 1998 High-temperature Superconductors: Materials, Properties and Applications (Dordrecht: Kluwer)

[10] Ogasawara T., 1989, Conductor design issues for oxide superconductors Part 1: criteria of magnetic stability, Cryogenics 29 3-5 https://doi.org/10.1016/0011-2275(89)90002-7

[11] Fietz W. et al, 1975, Superconducting Nb3Sn solenoids operating at 15 - 16.5 T, IEEE Trans. on Magn. 11 559-562 https://doi.org/10.1109/TMAG.1975.1058732

[12] Rosner C. H. et al, 1992, High field superconducting tape magnet technology, IEEE Trans. on Magn. 28 782-86 https://doi.org/10.1109/20.119994

[13] Wipf S. L., 1991, Review of stability in high temperature superconductors with emphasis on flux jumping, Cryogenics 31 936-48 https://doi.org/10.1016/0011-2275(91)90217-K

[14] Bruzzone P. et al, 2018, A Prototype Conductor by React&WIND Method for the EUROfusion DEMO TF Coils, IEEE Trans. on Appl. Supercond. 28 4202705 https://doi.org/10.1109/TASC.2017.2777939

[15] Takayasu M. et al, 2012, HTS twisted stacked-tape cable conductor, Supercond. Sci. Technol. 25 014011 http://dx.doi.org/10.1088/0953-2048/25/1/014011

[16] Grover F. W., 1946, Inductance Calculations: Working Formulas and Tables, Research Triangle Park, NC, USA: Instrum. Soc. Amer

[17] Dwight H. B., 1946, Geometric mean distances for rectangular conductors, Electrical Engineering 65 536–8 https://doi.org/10.1109/EE.1946.6434269

[18] Rosa E. B., 1908, The self and mutual-inductances of linear conductors, Bulletin of the Bureau of Standards

[19] Amemiya N., 1998, Overview of current distribution and re-distribution in superconducting cables and their influence on stability, Cryogenics 38 545-50 https://doi.org/10.1016/S0011-2275(98)00007-1

[20] Higashi Y. et al, 2019, Analysis of Magnetization Loss on a Twisted Superconducting Strip in a Constantly Ramped Magnetic Field, IEEE Trans. on Appl. Supercond. 29 8200207 https://doi.org/10.1109/TASC.2018.2874481

[21] Grilli F. et al, 2015, Numerical modeling of twisted stacked tape cables for magnet applications, Physica C: Superconductivity and its Applications 518 122-25 https://doi.org/10.1016/j.physc.2015.03.007

[22] Fukumoto Y. et al, 1995, Alternating-current losses in silver-sheathed (Bi,Pb)2Sr2Ca2Cu3O10 tapes II: Role of interfilamentary coupling, Appl. Phys. Lett. 67 3180 https://doi.org/10.1063/1.115155

[23] Campbell A., 1982, A general treatment of losses in multifilamentary superconductors, Cryogenics 22 3-16 https://doi.org/10.1016/0011-2275(82)90015-7

[24] Awaji S. et al, 2015, AC Losses of an HTS Insert in a 25-T Cryogen-Free Superconducting Magnet, IEEE Trans. on Appl. Supercond. 25 4601405 https://doi.org/10.1109/TASC.2014.2366552

[25] Kajikawa K. et al, 2016, AC loss evaluation of an HTS insert for high field magnet cooled by cryocoolers, Cryogenics 80 215-220 https://doi.org/10.1016/j.cryogenics.2016.05.010

[26] Grilli F. et al, 2016, How filaments can reduce AC losses in HTS coated conductors: a review, Supercond. Sci. Technol. 29 083002 https://doi.org/10.1088/0953-2048/29/8/083002

[27] Witz G. et al, 2002, Reduction of AC losses in Bi,Pb(2223) tapes by the introduction of barriers and the use of new wire configurations, Physica C: Superconductivity 372-376 1814-7 https://doi.org/10.1016/S0921-4534(02)01133-4

[28] Stavrev S. et al, 2003, AC Losses of Multifilamentary Bi-2223/Ag Conductors With Different Geometry and Filament Arrangement, IEEE Trans. on Appl. Supercond. 13 3561-65 https://doi.org/10.1109/TASC.2003.812398

[29] Bykovsky N. et al, 2017, Cyclic load effect on round strands made by twisted stacks of HTS tapes, Fusion Engineering and Design 124 6-9 http://dx.doi.org/10.1016/j.fusengdes.2017.04.050

[30] Pardo E. et al, 2004, The transverse critical-state susceptibility of rectangular bars, Supercond. Sci. Technol. 17 537 http://stacks.iop.org/SUST/17/537

[31] Bykovsky N. et al, 2016, Magnetization loss for stacks of ReBCO tapes, Supercond. Sci. Technol. 30 024010 http://dx.doi.org/10.1088/1361-6668/30/2/024010

[32] Awaji S. et al, 2013, New 25 T Cryogen-Free Superconducting Magnet Project at Tohoku University, IEEE Trans. on Appl. Supercond. 24 4302005 https://doi.org/10.1109/TASC.2013.2292367

[33] Takahashi M. et al, 2017, Design and Test Results of a Cryogenic Cooling System for a 25-T Cryogen-Free Superconducting Magnet, IEEE Trans. on Appl. Supercond. 27 4603805 https://doi.org/10.1109/TASC.2017.2673762

[34] Wang L. et al, 2016, The Effect of Temperature Dependence of AC Losses in a Bi-2223/Ag Insert of an 8-T Superconducting Magnet, IEEE Trans. on Appl. Supercond. 26 4702605 https://doi.org/10.1109/TASC.2016.2536947

[35] 2018 Berrospe-Juarez Estimation of Losses in the (RE)BCO Two-Coil Insert of the NHMFL 32 T All-Superconducting Magnet IEEE Trans. on Appl. Supercond. 28 4602005   https://doi.org/10.1109/TASC.2018.2791545

[36] Hahn S. et al, 2015, Construction and Test of 7-T/68-mm Cold-Bore Multiwidth No-Insulation GdBCO Magnet, IEEE Trans. on Appl. Supercond. 25 4600405 https://doi.org/10.1109/TASC.2014.2363555

[37] Durante M. et al, 2018, Realization and First Test Results of the EuCARD 5.4-T REBCO Dipole Magnet, IEEE Trans. on Appl. Supercond. 28 4203805 https://doi.org/10.1109/TASC.2018.2796063

[38] Sogabe Y. et al, 2016, Influence of magnetization on field quality in cosine-theta and block design dipole magnets wound with coated conductors, Supercond. Sci. Technol. 29 045012 https://doi.org/10.1088/0953-2048/29/4/045012

[39] Pardo E. et al, 2012, AC loss in ReBCO pancake coils and stacks of them: modelling and measurement, Supercond. Sci. Technol. 25 035003 http://stacks.iop.org/SUST/25/035003

[40] Wang M. et al, 2019, Study on the Screening Current Induced Field of a Novel Narrow HTS Tape with 1 mm Width, IEEE Trans. on Appl. Supercond. 29 6601905 https://doi.org/10.1109/TASC.2019.2902420

[41] Solovyov V. et al, 2019 Performance of layer wound epoxy impregnated coils made from a multifilamentary cable of exfoliated YBCO, Supercond. Sci. Technol. 32 054006 https://doi.org/10.1088/1361-6668/ab0b9c

[42] Hase et al, 1994,   A.c.. losses in Bi-2212 superconducting magnet at 20 K, Cryogenics 34 603-607 https://doi.org/10.1016/0011-2275(94)90187-2

[43] Hale J. R. et al, 1968, The Transient Stabilization of Nb_3Sn Composite Ribbon Magnets, Journal of Applied Physics 39 2634 https://doi.org/10.1063/1.1656640

[44] Rosner C. H. et al, 1992, High field superconducting tape magnet technology, IEEE Trans. on Appl. Supercond. 28 782-86 https://doi.org/10.1109/20.119994

[45] Dembrowska A. et al, 2018, Thermal-Hydraulic Analysis of the DEMO CS Coil, IEEE Trans. on Appl. Supercond. 28 4205605 https://doi.org/10.1109/TASC.2018.2809425

[46] Bykovsky N. et al, 2018, AC Loss in HTS Fusion Cables: Measurements, Modeling, and Scaling Laws, IEEE Trans. on Appl. Supercond. 28 5900305 https://doi.org/10.1109/TASC.2018.2803264

[47] Wesche R. et al, 2018, DEMO Central Solenoid Design Based on the Use of HTS Sections at Highest Magnetic Field, IEEE Trans. on Appl. Supercond. 28 4203605 https://doi.org/10.1109/TASC.2018.2797955

[48] Pardo E. et al, 2002, Magnetic properties of arrays of superconducting strips in a perpendicular field, Phys. Rev. B 67 104517 https://doi.org/10.1103/PhysRevB.67.104517

[49] Yanagi N et al 2016 Magnet design with 100-kA HTS STARS conductors for the Helical Fusion Reactor Cryogenics 80 243–9 http://dx.doi.org/10.1016/j.cryogenics.2016.06.011

[50] Bansal et al. 2008, High-Temperature Superconducting Coil Option for the LHD-Type Fusion Energy Reactor FFHR, Plasma and Fusion Research: Regular Articles 3 S1049 https://doi.org/10.1585/pfr.3.S1049

[51] Whyte D., 2019, Small, modular and economically attractive fusion enabled by high temperature superconductors, Phil. Trans. R. Soc. A 377 20180354 http://dx.doi.org/10.1098/rsta.2018.0354

[52] Windridge M., 2019, Smaller and quicker with spherical tokamaks and high-temperature superconductors, Phil. Trans. R. Soc. A 377 20170438 http://dx.doi.org/10.1098/rsta.2017.0438

Highlights

- HTS cable designs imitates LTS cable designs, despite the radical difference in properties (for example stability, temperature margin, mechanical limits) between HTS and LTS.

- Inductance mismatch (causing current re-distributions) and AC losses have been studied by numerical and analytical methods in twisted and non-twisted stacks of coated conductors; various experiments reported in the literature support the analysis.

- Large losses (hysteretic losses) are common to all magnets built with tapes. Large AC fields (larger than the penetration field) should be applied to measure the losses in conditions relevant to applications.

- Hysteretic losses in twisted stack of tapes are marginally lower than the saturated losses of non-twisted stacks. Therefore, twisting a stack of tapes has modest effect on AC losses.

- It is ineffective to twist stacks of HTS tapes, because stability, inductance and AC losses are only marginally affected by twisting.

- In general, HTS magnet design should be rigorously motivated by physical analysis, not simply copied from past LTS magnets.

Davide Uglietti: conceiving the idea, writing manuscript, analytical calculations.

Rui Kang: numerical calculation in section 2, reviewing

Francesco Grilli: verified loss calculation, reviewing and editing

Rainer Wesche: reviewing (especially section 1) and editing